Apical targeting and endocytosis of the sialomucin endolyn are essential for establishment of zebrafish pronephric kidney function

Di Mo[1], Gudrun Ihrke[2], Simone A. Costa[3], Lauren Brilli[4,5], Anatália Labilloy[1], Willi Halfter[6], Chiara Cianciolo Cosentino[4], Neil A. Hukriede[4] and Ora A. Weisz[1,7,*]

[1]Renal Electrolyte Division, and [4]Department of Developmental Biology, and [5]Medical Scientist Training Program, and [6]Department of Neurobiology, and [7]Department of Cell Biology and Physiology, University of Pittsburgh School of Medicine, Pittsburgh, PA 15261, USA
[2]Department of Pharmacology, Uniformed Services University School of Medicine, Bethesda, MD, USA
[3]Department of Biological Sciences, Carnegie Mellon University, Pittsburgh, PA 15213, USA
*Author for correspondence (weisz@pitt.edu)

Accepted 6 August 2012
Journal of Cell Science 125, 5546–5554

doi: 10.1242/jcs.111468

Summary

Kidney function requires the appropriate distribution of membrane proteins between the apical and basolateral surfaces along the kidney tubule. Further, the absolute amount of a protein at the cell surface versus intracellular compartments must be attuned to specific physiological needs. Endolyn (CD164) is a transmembrane protein that is expressed at the brush border and in apical endosomes of the proximal convoluted tubule and in lysosomes of more distal segments of the kidney. Endolyn has been shown to regulate CXCR4 signaling in hematopoietic precursor cells and myoblasts; however, little is known about endolyn function in the adult or developing kidney. Here we identify endolyn as a gene important for zebrafish pronephric kidney function. Zebrafish endolyn lacks the N-terminal mucin-like domain of the mammalian protein, but is otherwise highly conserved. Using *in situ* hybridization we show that endolyn is expressed early during development in zebrafish brain, eye, gut and pronephric kidney. Embryos injected with a translation-inhibiting morpholino oligonucleotide targeted against endolyn developed pericardial edema, hydrocephaly and body curvature. The pronephric kidney appeared normal morphologically, but clearance of fluorescent dextran injected into the common cardinal vein was delayed, consistent with a defect in the regulation of water balance in morphant embryos. Heterologous expression of rat endolyn rescued the morphant phenotypes. Interestingly, rescue experiments using mutant rat endolyn constructs revealed that both apical sorting and endocytic/lysosomal targeting motifs are required for normal pronephric kidney function. This suggests that both polarized targeting and postendocytic trafficking of endolyn are essential for the protein's proper function in mammalian kidney.

Key words: MDCK, Apical, Kidney development, Polarity

Introduction

Morphogenesis and homeostasis of epithelia require the coordination of cell differentiation, proliferation, survival, migration, adhesion, and polarization. Differentiated epithelial cells further respond to changes in their environment by adjusting the compositions of their two different plasma membrane domains to fulfil vectorial transport functions as needed. This is achieved through the appropriate integration of activated signaling pathways upon cues cells receive from their environment. The sialomucin endolyn (CD164) is a highly glycosylated membrane protein that has recently been described as a novel regulator of cell signaling in non-renal tissues. In hematopoietic precursor cells, myoblasts, and various epithelial-derived cancer cells, endolyn associates with the chemokine receptor CXCR4 and regulates downstream signaling and cell behavior, such as collective cell migration (Bae et al., 2008; Forde et al., 2007; Havens et al., 2006; Lee et al., 2001; Tang et al., 2012). Endolyn is highly expressed in mammalian kidney both in embryos and adults, and it is frequently upregulated in renal cell cancer (Jones et al., 2005). We have previously shown that the protein is targeted to the apical cell surface in renal epithelial cells and cycles between plasma membrane and lysosomes (Ihrke et al., 2001; Ihrke et al., 2004; Potter et al., 2006); however, little is known about its function in this cell type. CXCR4 is expressed at low or undetectable levels in fully differentiated renal cells suggesting that endolyn may also regulate downstream signaling of other signaling receptors, or operate via completely different mechanisms (Eitner et al., 1998; Tögel et al., 2005).

In this study, we made use of the zebrafish model to begin to shed light on the importance of endolyn function in renal cells. The zebrafish *Danio rerio* has emerged as an attractive model system in which to study vertebrate renal development and function (Drummond, 2005; Swanhart et al., 2011; Wingert and Davidson, 2008). The zebrafish pronephric kidney contains only two nephrons with similar tubular segmentation and cell types found in the mammalian kidney (Wingert and Davidson, 2008). Moreover, filtration and osmoregulation can be measured in the pronephric kidney by 48 hours post-fertilization (hpf), allowing early assessment of kidney function (Cianciolo Cosentino et al., 2010; Drummond and Davidson, 2010; Hentschel et al., 2005).

Several important domains have been identified in endolyn. The luminal domain contains two mucin-like domains separated by a cysteine-rich domain (Ihrke et al., 2000). We have previously shown that an N-glycan-dependent epitope in the cysteine-rich domain mediates sorting of endolyn to the apical surface of renal epithelial cells (Ihrke et al., 2001; Potter et al., 2004). Among all vertebrate endolyn proteins the transmembrane and short cytosolic domains are nearly identical and contain a tyrosine-based trafficking motif at their carboxy-terminus that mediates endocytosis and lysosomal sorting (Ihrke et al., 2001; Ihrke et al., 2000; Ihrke et al., 2004). The N-terminal mucin-like domain of mammalian endolyn, which is thought to be required for adhesion of hematopoietic precursor cells to bone marrow stroma and effect cell proliferation (Altschuler et al., 2000; Doyonnas et al., 2000; Zannettino et al., 1998), is absent in lower vertebrate species such as zebrafish.

Using a translation-blocking morpholino (MO) we knocked down endolyn expression in zebrafish embryos to interrogate whether acute loss of endolyn interfered with pronephric kidney development or function. We found that endolyn is expressed early during development and localized to the kidney, brain and digestive tract within several hours after fertilization. Endolyn knockdown revealed a developmental phenotype consistent with a defect in pronephric kidney function. This phenotype was fully rescued by heterologous expression of rat endolyn. However, mutation of either the apical targeting signal or the critical tyrosine residue required for endolyn endocytosis and lysosomal targeting prevented rescue. Our study shows that endolyn expression is needed for normal pronephros function, but its absence does not inhibit pronephros formation per se. It further emphasizes the efficacy of the zebrafish model in highlighting essential motifs and domains involved in protein function during development.

Results

Dual localization of endolyn in mammalian adult kidney

Our previous studies in Madin Darby Canine Kidney (MDCK) type II cells demonstrated that endolyn has an unusual trafficking pattern in that the newly synthesized protein is targeted to the apical surfaces, where it is internalized and transported to lysosomes (Ihrke et al., 2001). It continues to recycle between lysosomes and the cell surface (Cresawn et al., 2007; Potter et al., 2006), but relatively little endolyn is found at the cell surface in this model system at steady state (Ihrke et al., 2001). In rat kidney, endolyn is also found primarily in lysosomes in proximal straight and distal tubules and the collecting system (supplementary material Fig. S1). However, in proximal convoluted tubule a significant fraction of endolyn localizes to the brush border (Fig. 1), suggesting differential functions along the kidney tubule.

Expression of endolyn in zebrafish embryos

Zebrafish endolyn is 43% identical to the rat protein. All domains are highly conserved except the N-terminal mucin-like domain, which is absent. Four of 8–9 potential N-glycosylation sites lie within the cysteine-rich region that contains the N-glycan dependent apical targeting motif characterized in rat endolyn (Fig. 2). The eight cysteines defining the structure of this domain are all conserved between mammals and lower vertebrates. The transmembrane and cytoplasmic sequences are almost identical,

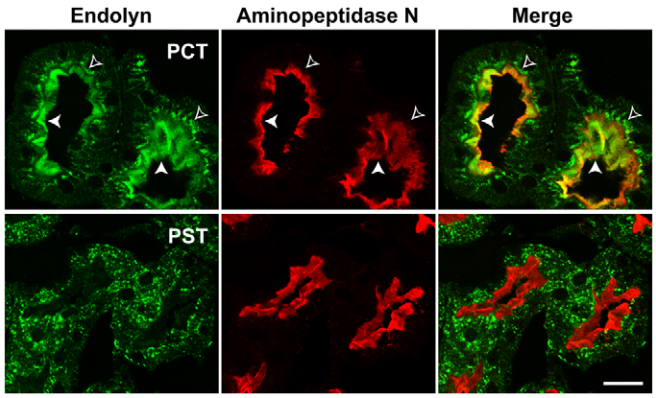

Fig. 1. Endolyn is differentially localized along the rat kidney tubule. Adult rat kidney sections were co-labelled with antibodies to endolyn (green) and the proximal tubule marker aminopeptidase N (red), which strongly labels the apical brush border. Endolyn localizes prominently to the brush border of proximal convoluted tubules (PCT, upper panel), indicated by filled arrowheads; open arrowheads point to intracellular subapical endosomes. By contrast, endolyn is primarily intracellular in proximal straight tubules (PST, lower panel) and subsequent segments (see also supplementary material Fig. S1). Scale bar: 20 μm.

with one conservative amino acid change in each domain, and end with the endocytosis motif YHTL.

RT-PCR confirmed the expression of endolyn as early as the 10 somite stage (ss; Fig. 3A). We next conducted whole mount *in situ* hybridization to examine the expression of endolyn at different developmental stages (Fig. 3B). Endolyn was expressed in the brain and the developing pronephric kidney by the 13 ss, and strong staining persisted through 72 hpf. At 72 hpf, endolyn was also observed in the digestive system. The localization of

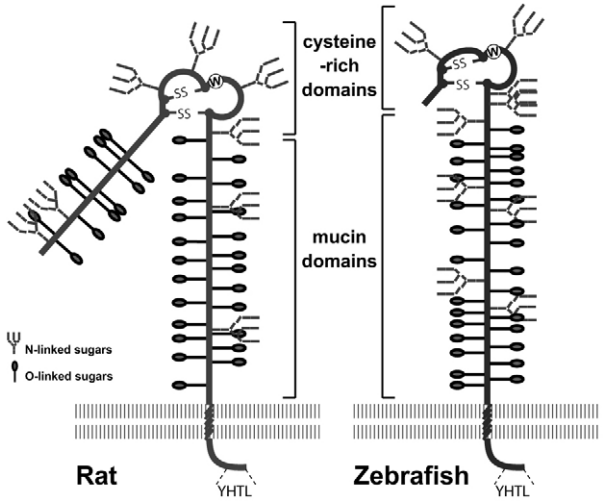

Fig. 2. Schematic drawings of rat and zebrafish endolyn. Rat endolyn contains two highly O-glycosylated mucin-like domains separated by a cysteine-rich domain. Zebrafish endolyn contains only the membrane-proximal mucin-like domain. The cysteine-rich domains of both endolyn orthologs carry at least two conserved N-glycosylation sites. The transmembrane and cytosolic domains are identical except for two conserved substitutions. The locations of potential N-glycosylation sites and predicted O-glycosylation sites (NetOglyc3.1 program, www.cbs.dtu.dk/services/NetOGlyc/ (Julenius et al., 2005)] are marked.

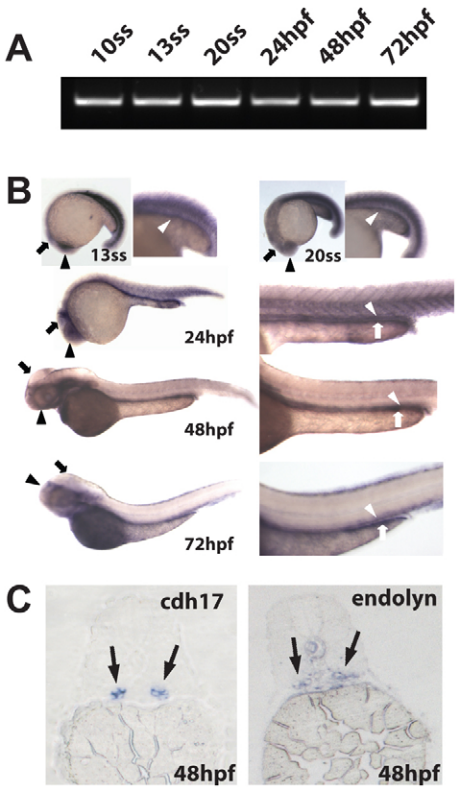

Fig. 3. Endolyn is expressed in the zebrafish kidney, brain and digestive system. (**A**) RT-PCR analysis of RNA extracted from embryos at the indicated stages was performed using specific primers against endolyn. All lanes show a band of the expected size (~600 bp). (**B**) *In situ* hybridization for endolyn in embryos was performed at 13 ss and 20 ss and at 24, 48, 72 hpf. Kidney (white arrowhead), brain (black arrow) and eye (black arrowhead) staining are evident by the 13 ss stage and staining of the digestive system (white arrow) appears by 24 hpf. (**C**) Cross sections through the proximal tubule of zebrafish embryos at 48 hpf (5 μm) were stained by *in situ* hybridization using probes to cadherin 17 (cdh17), a pronephric marker, or endolyn. Endolyn staining coincided with that of cadherin 17 in the expected region, confirming endolyn localization in the pronephric kidney.

endolyn in embryo cross-sections was comparable to that of the pan kidney marker cadherin 17 (cdh17), confirming localization of the transcript to the pronephric kidney at 48 hpf (Fig. 3C).

To determine the subcellular distribution of endolyn in zebrafish larvae, we injected mRNA encoding rat endolyn into embryos and fixed at 48 hpf. We used a polyclonal antibody recognizing the luminal domain of rat endolyn for detection by indirect immunofluorescence, which did not cross react with endogenous endolyn (not shown). Some sections were double labelled with the monoclonal antibody 3G8, which labels the apical surface of the pronephric kidney proximal tubule. Rat endolyn colocalized with the 3G8 antigen in the pronephric tubule (Fig. 4), consistent with apical targeting of the protein in zebrafish. Additionally, apical endolyn staining was also detected along the lumen of the gut.

Knockdown of endolyn disrupts pronephric kidney function

To elucidate the role of endolyn in zebrafish development, we injected a translation blocking MO to knock down endolyn

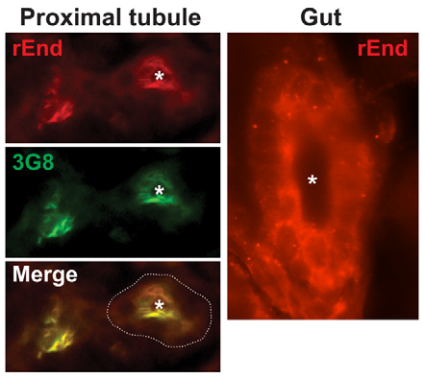

Fig. 4. Rat endolyn is targeted to the apical surface of the zebrafish proximal tubule. mRNA encoding wild-type rat endolyn (200 ng) was injected into zebrafish embryos at the one-cell stage. Embryos were fixed at 48 hpf, sectioned and incubated with polyclonal anti-rat endolyn (rEnd) and monoclonal 3G8 antibodies (to mark the apical surface of proximal tubules) as described in Materials and Methods. Cross sections through the proximal tubule and gut are shown. The periphery of the proximal tubule is outlined in the merged image and the lumen is marked by an asterisk.

expression. By 48 hpf, the endolyn-depleted embryos were developmentally impaired and exhibited pericardial edema, hydrocephaly, and abnormal body curvature (Fig. 5A). Embryos were classified as wild type, mild-to-moderately affected (class I) and severely affected or dead (class II) based on the extent of body curvature and edema (Fig. 5B). Injection of 5 ng MO resulted in moderate to severe phenotypes in ~70% of embryos by 48 hpf, whereas ~90% of the embryos injected with a scrambled control MO developed normally. The severity of the phenotype was dose dependent. Approximately 10, 30, 70 and 95% of embryos injected with 2.5, 5, 7.5 and 10 ng MO, respectively, were categorized as having severe phenotypes (Fig. 5B). For subsequent experiments, we injected embryos with 5 ng MO and selected mild-to-moderately affected larvae for morphological and functional analysis.

We next compared the organization of the pronephric kidney in embryos injected with control or endolyn MO. *In situ* hybridization was performed at 48 hpf using the pan pronephric marker cdh17 as well as markers selective for podocytes (wt1a), the proximal tubule (slc4a4) and the distal tubule (slc12a1). No gross defects in kidney structure were observed in endolyn morphants compared with controls, indicating that endolyn is not required for morphogenesis of the zebrafish pronephros (Fig. 6). Moreover, cell polarity was not compromised, as the cellular polarity of the basolateral marker Na^+K^+-ATPase was unaffected in morphants (supplementary material Fig. S2A). We routinely observed dilated tubules and more intense staining in morphants with all probes, but the overall segmental pattern was never changed. Tubule dilation in endolyn morphants was not due to obstruction, as the tubular lumen was patent and the cloaca was open (supplementary material Fig. S2B,C).

To examine whether pronephric kidney function was compromised by endolyn depletion, we performed a rhodamine-dextran clearance assay. 1 ng of 10 kDa rhodamine-dextran was injected into the common cardinal vein of class I embryos at 48 hpf and depletion of fluorescence at the injection site was monitored over time (1–24 h post-injection) as a

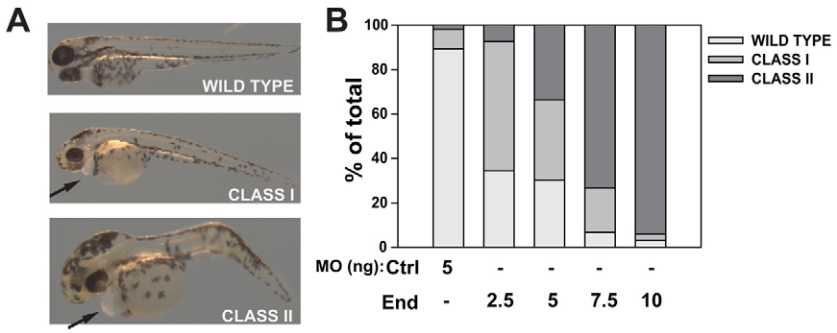

Fig. 5. Endolyn morphants develop pericardial edema, hydrocephaly, and body curvature. (**A**) Zebrafish larvae were imaged 48 hpf after endolyn MO injection and classified as wild type (no visible pericardial edema or body curvature), moderately affected (Class I: frank pericardial edema, visible body curvature, hydrocephaly) and severely affected or dead (Class II: severe pericardial edema, body curvature, severe hydrocephaly). Representative images from each class are shown. (**B**) The distribution of observed phenotypes at 48 hpf in embryos injected with control (Ctrl) MO or the indicated doses of endolyn (End) MOs is graphed. Endolyn knockdown elicits concentration-dependent effects on larval edema and survival. Three independent injections were quantified with 50 or more injected embryos per condition in each experiment.

measure of renal clearance. Rhodamine-dextran was efficiently cleared from larvae injected with control-MO but clearance was significantly slowed in endolyn-MO injected larvae, consistent with a defect in osmoregulation (Fig. 7A,B). Defective clearance was not due to altered cardiac function, as the heart rate of control embryos and class I morphants was not significantly different (101±13 beats per min for control versus 91±13 for morphants, $n=20$).

Dextran clearance from the tubule occurs in part by its endocytosis in the proximal pronephric duct (Anzenberger et al., 2006; Drummond and Davidson, 2010; Hentschel et al., 2005). To determine whether endocytosis was compromised in endolyn morphants, we followed the clearance and endocytosis of 70 kDa rhodamine dextran after injection into the common cardinal vein at 48 hpf. At this point in embryonic development, the glomerular filtration barrier is not fully formed and like 10 kDa dextran, this larger tracer readily enters the pronephric kidney tubule. Similar to our results using the 10 kDa tracer, clearance of 70 kDa dextran was significantly reduced in class I morphants compared to control (not shown; $P<0.001$ at 5 h and 24 h post-injection). Uptake of fluorescence dextran into endocytic vesicles lining the proximal pronephric duct could be readily visualized in control embryos (Fig. 7C). In contrast, no uptake of rhodamine-dextran was evident in class I morphants, demonstrating that depletion of endolyn interferes with normal endocytosis and disrupts the function of the pronephric kidney (Fig. 7C).

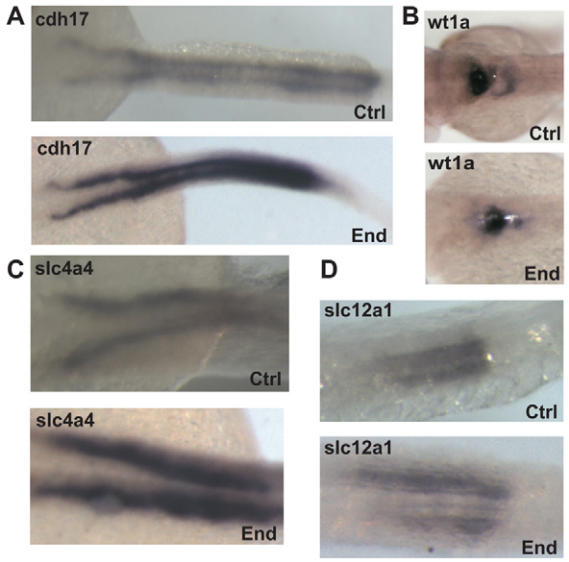

Fig. 6. Kidney morphology is intact after endolyn knockdown. (**A**) In situ hybridization was performed at 48 hpf to detect cdh17 expression in embryos injected with either control (Ctrl) or endolyn (End) MOs. (**B–D**) In situ hybridization was performed at 48 hpf in embryos injected with either control or endolyn MO to detect markers for podocytes (wt1a) (B), proximal tubule (slc4a4) (C), and distal tubule (slc12a1) (D). The morphology of the pronephric kidney in morphants is not grossly disrupted, although the tubules appear dilated. Class I morphants were used in all experiments.

Rat endolyn efficiently restores endolyn function during pronephric kidney development

To exclude any off-target effects of the endolyn MO, we asked whether heterologous expression of mRNA encoding rat endolyn could rescue the developmental defects we observed in endolyn MO-injected larvae. First, we tested the effect of injecting rat endolyn mRNA without concomitant MO injection. Delivery of up to 300 pg rat endolyn mRNA into zebrafish larvae did not cause developmental defects, suggesting that overexpression of endolyn is not detrimental to the embryos (Fig. 8). Strikingly, we found that injection of 200 pg mRNA encoding wild-type rat endolyn was sufficient to rescue the endolyn MO phenotype. Whereas only ~30% of embryos injected with 5 ng endolyn MO were classified as normal or mildly affected, injection of 200 pg rat endolyn mRNA restored normal development in ~90% of larvae. Injection of 100 pg resulted in ~75% of embryos developing normally (Fig. 9D).

Lumenal and cytoplasmic regions are required for endolyn function in the pronephric kidney

To identify the critical domain(s) for endolyn function in zebrafish pronephros, we generated rat endolyn constructs containing mutations within the lumenal, transmembrane, or cytoplasmic domains for use in rescue experiments (see schematic in Fig. 9A). To examine the requirement for apical sorting in endolyn function during zebrafish development, we

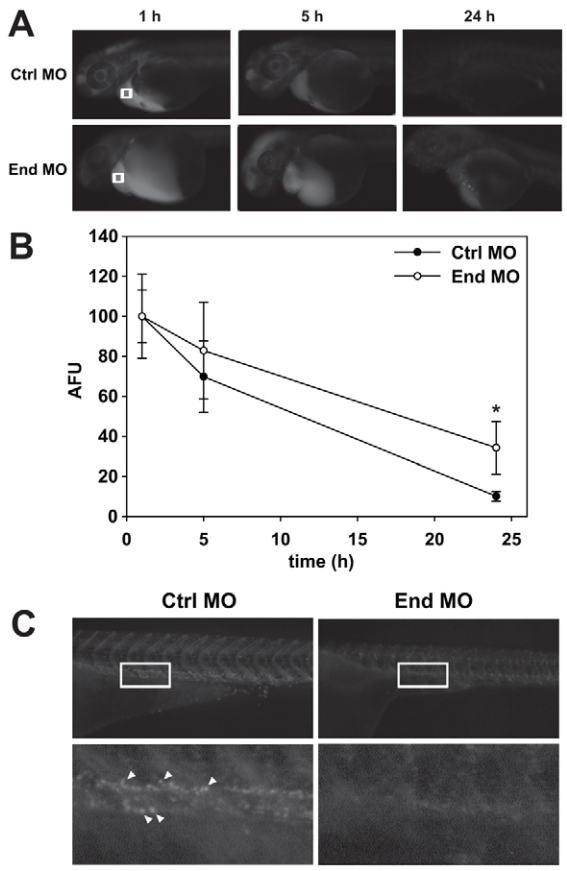

Fig. 7. Pronephric kidney function is disrupted in endolyn morphants. (**A**) 1 ng of 10 kDa rhodamine-dextran was injected into the common cardinal vein of control (Ctrl) or endolyn (End) morphants at 48 hpf. Images were acquired under identical conditions at 1, 5 and 24 h post-injection. (**B**) The loss of fluorescence over time near the common cardinal vein (regions marked by white boxes in A) was quantified, normalized to the initial fluorescence observed at 1 h, and plotted. Three independent injections were quantified with at least ten Class I and control embryos injected in each experiment. At 24 h, retained fluorescence is significantly greater in endolyn morphants compared with controls (*P=0.001 by Mann–Whitney rank sum test). (**C**) Imaging of the pronephric proximal tubule 24 h after injection of 70 kDa rhodamine-dextran demonstrates impaired endocytosis in endolyn morphants. Bottom panels show enlarged regions of the areas delineated by white rectangles in the corresponding upper panels. Arrowheads point to examples of endocytic vesicles in control larvae.

prevented N-glycosylation of the cysteine-rich domain by mutating the four key asparagine residues to alanine (4NA). We confirmed the polarity of overexpressed proteins in stably transfected MDCK cells. Indirect immunofluorescence labelling showed that wild-type endolyn was largely confined to the apical surface at steady state, whereas the 4NA mutant was also observed at the basolateral membrane (Fig. 9B). To verify that newly synthesized 4NA was partially missorted, we performed domain-selective biotinylation of radiolabelled cells (Fig. 9C). Only 63% of the 4NA mutant at the cell surface was delivered apically, compared with 83% of wild-type endolyn. This reduction in polarity is consistent with our previous results using similar glycosylation mutants (Potter et al., 2004).

Injection of 100 pg of mutant 4NA mRNA failed to restore normal development of morphant zebrafish embryos (Fig. 9D).

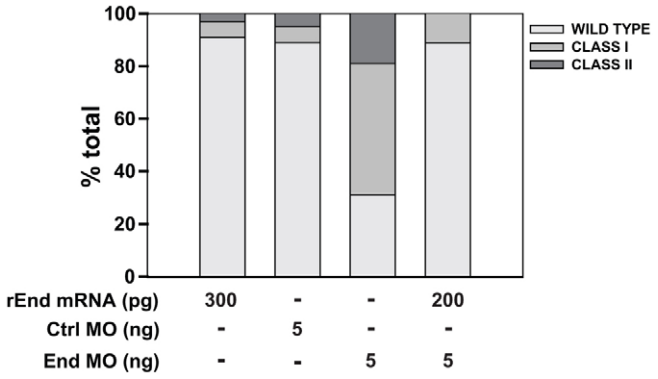

Fig. 8. Heterologous expression of rat endolyn restores endolyn function during kidney development. Embryos were injected with 300 pg of mRNA encoding rat endolyn (rEnd) and evaluated at 48 hpf. For rescue experiments, embryos were injected (or not) with 200 pg rEnd mRNA followed by injection with 5.0 ng control or endolyn (End) MO, and phenotypes were classified at 48 hpf. Data are combined from three experiments with 50 or more embryos per condition.

Essentially identical results were obtained when a mutant construct in which the entire lumenal domain of endolyn was replaced by the corresponding region of CD8 (not shown). These data suggest that endolyn's lumenal domain, and more specifically the glycan-dependent apical targeting information, is critical for its function in zebrafish kidney development. Importantly, even a modest level of endolyn missorting seems to be sufficient to prevent proper functioning.

The transmembrane domain of endolyn contains a five amino acid motif (FIGGI) that is completely conserved among species. To test the role of this sequence in endolyn function, we expressed the mutant TMD3, in which the phenylalanine and two glycine residues were conservatively substituted by leucine and alanines, respectively. This mutant was apically delivered similar to wild-type endolyn in MDCK cells as assessed by indirect immunofluorescence and domain selective biotinylation (Fig. 9B,C). The ability of this mutant to rescue endolyn morphants was also comparable to wild-type rat endolyn, suggesting that endolyn is fully functional in the absence of the FIGGI motif (Fig. 9D).

Finally, we examined a mutant that lacks the cytoplasmic tyrosine critical for endocytosis and lysosomal sorting of endolyn (YA). Similar to the 4NA mutant, expression of this construct was unable to rescue the morphant phenotype (Fig. 9D). This suggests that apical sorting of endolyn and its distribution between surface and intracellular compartments are similarly important for endolyn function during early development.

To confirm that expression of rat endolyn also restored renal function in endolyn morphants, we monitored dextran clearance efficiency in embryos co-injected with endolyn MO and either wild type or mutant rat endolyn mRNA. As predicted, clearance of 10 kDa rhodamine dextran in morphants expressing wild-type rat endolyn was equivalent to that in control embryos (supplementary material Fig. S3). Similarly, the TMD3 mutant also fully restored dextran clearance efficiency. In contrast, expression of 4NA or YA mutant constructs were unable to correct the defect in dextran clearance in endolyn morphants (supplementary material Fig. S3). Together, these data indicate that endolyn expression at the apical surface of renal epithelial

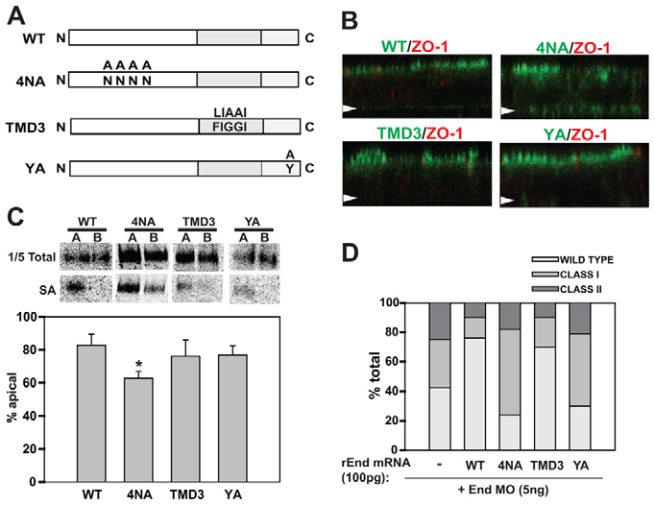

Fig. 9. Lumenal and cytoplasmic domains of rat endolyn are required for its function during pronephric development. (**A**) Schematic of rat endolyn mutants used for rescue studies. The 4NA mutant lacks consensus sites for addition of the four N-glycans within the cysteine-rich region. TMD3 contains three mutations within the highly conserved FIGGI sequence within the transmembrane region. The YA mutant contains a tyrosine-to-alanine substitution that disrupts the endocytic/lysosomal targeting motif at the carboxy terminus. (**B**) Filter-grown MDCK cells stably expressing either wild-type endolyn or the various mutants were fixed and processed for indirect immunofluorescence to detect endolyn (green) and the tight junction marker ZO-1 (red). Cells were visualized by confocal microscopy and representative XZ sections are shown. The position of each filter is marked with an arrow. (**C**) Filter-grown MDCK cells stably expressing wild-type or mutant rat endolyn were radiolabelled with [^{35}S]-cysteine for 2 h, then chased for 1 h. Cells were biotinylated either apically (A) or basolaterally (B) and cells were solubilized and immunoprecipitation with anti-endolyn antibody. After elution, one-fifth of each sample was reserved as total and the remainder was incubated overnight with streptavidin agarose (SA) to recover surface proteins. Representative gels are shown for each sample and the results from three independent experiments are plotted. The polarity of 4NA is statistically different from wild type (*$P<0.001$ by Student's *t*-test) and from YA and TMD3 mutants ($P<0.02$ and $P=0.024$, respectively). The polarity of TMD3 and YA was not significantly different from wild type or each other. (**D**) mRNA encoding wild-type or mutant rEnd constructs (100 pg) was injected into zebrafish embryos at the one-cell stage, followed by injection of 5 ng of endolyn morpholino. Images were acquired at 48 hpf and morphant phenotypes were classified and quantified. Data are combined from three experiments with 50 or more embryos per condition.

cells and its endocytosis from this surface is crucial to the proper functioning of the developing zebrafish kidney.

Discussion

In these studies we have identified a novel role for the sialomucin endolyn during zebrafish development and establishment of a functional pronephric kidney. Endolyn is expressed as early as the 10-somite stage in zebrafish embryos and persists in the kidney, brain, and digestive system at least through 72 hpf. Kidney organogenesis and organization were not grossly disrupted upon endolyn knockdown using a translation blocking morpholino. However, morphants exhibited pericardial edema, visible body curvature and hydrocephaly, consistent with a water balance defect indicating a potential kidney malfunction. Moreover, we observed tubular dilation and a reduced rate of clearance of 10 KDa rhodamine-dextran in morphants. The morphant phenotype could be fully rescued by heterologous expression of rat endolyn, which was targeted apically to zebrafish epithelial lumens. However, endolyn mutants lacking the glycan-dependent apical targeting signal or the endocytic/lysosomal targeting motif did not restore normal development and pronephros function. These data suggest that efficient apical delivery and endocytosis are both required for proper endolyn function in the pronephric kidney.

Intact lumenal and cytoplasmic domains are required for endolyn function

Endolyn has been studied extensively in polarized epithelial cells *in vitro* as an apically targeted glycoprotein with N-glycosylation-dependent sorting information. Apical sorting of endolyn relies on terminal processing of two N-glycans within the cysteine-rich region of the lumenal domain (Potter et al., 2004). In polarized MDCK cells, this apical signal is dominant over basolateral sorting information such that newly synthesized endolyn is delivered primarily to the apical surface. Subsequently, it is internalized and delivered to lysosomes (Ihrke et al., 2001). The proportion of radiolabelled endolyn present at the apical surface remains steady for up to 21 h after labelling, suggesting that endolyn cycles constitutively between lysosomes and the cell membrane (Potter et al., 2006). Mutation of the critical tyrosine residue in the endocytic/lysosomal targeting motif prevents binding to adaptor protein complexes and enhances surface expression of the protein (Ihrke et al., 2004). Interestingly, expression of mutants lacking either N-glycosylation consensus sequences required for polarized sorting or an intact endocytic motif could not rescue the endolyn morphant phenotype, whereas heterologous expression of wild-type rat endolyn restored the normal morphology. In contrast, disruption of a highly conserved sequence within the transmembrane domain of endolyn did not inhibit efficient rescue by rat endolyn. The fact that both trafficking motifs are indispensable for rescue suggests that proper modulation of endolyn's distribution between the (apical) cell surface and endosomal/lysosomal compartments is a key requirement for endolyn function. Moreover, the reduced dextran uptake in kidneys of endolyn MO-treated zebrafish suggests that endolyn is actively involved in the regulation of some endocytic mechanism(s).

The observation that disrupting the N-glycan-dependent apical sorting motif of endolyn prevented rescue of the morphant phenotype was somewhat unexpected, given that the protein is still delivered to the cell surface with a slight apical preference. Compared with wild-type endolyn, where roughly 83% of the newly synthesized protein is delivered apically, we found that 63% of 4NA was present at the apical surface under similar labelling conditions. There are two possible explanations for this observation. First, missorting of a fraction of 4NA to the basolateral surface may be sufficient to disrupt rescue by this mutant. A precedence for the inverse scenario is presented by a disease-causing mutant form of the anion exchanger AE1 lacking a basolateral sorting motif (Devonald et al., 2003). However, in this case it is clear that any missorting to the wrong surface will disturb the balance of ion transport across the renal epithelium. While it is conceivable that endolyn effects the distribution of other membrane proteins, it itself is unlikely to have any ion transport activity. However, lowering the effective endolyn

concentration at the apical plasma membrane may be sufficient to disrupt its normal physiology. Alternatively, the N-glycans within the cysteine-rich domain may serve another function in addition to their role in apical targeting. These N-glycans may be important for association of endolyn with other protein(s) on the same membrane or extracellular ligands. Given the apparent requirement for endolyn internalization and lysosomal targeting, it is tempting to speculate that endolyn-mediated binding and endocytosis of an associated ligand or *cis*-receptor may be important for its function. Similar to other sialomucins, endolyn is thought to mediate cell-cell (or cell-matrix) adhesion (Doyonnas et al., 2000; Zannettino et al., 1998); however, no membrane-bound ligand has yet been identified. Noteworthy, the N-terminal mucin-like domain of mammalian endolyn, which has been implicated in cell adhesion (Doyonnas et al., 2000), is not present in zebrafish endolyn and therefore not expected to be required for rescue of the knockdown phenotype in zebrafish.

A detailed comparison of endolyn expression during zebrafish and mammalian development is currently not possible due to the lack of sufficient data; however, similarities clearly exist. Images in the Allen Developing Mouse Brain Atlas of embryonic day (E) 11.5 mouse embryos show significant endolyn expression in a variety of epithelial tissues and some expression in medullary hindbrain (Allen Institute for Brain Science, http://developingmouse.brain-map.org/). Prominent expression is observed in the developing metanephric kidney at E13.5. Different from zebrafish, endolyn is well expressed in the somites of mouse embryos, which give rise to skeletal muscle cell precursors (Bae et al., 2008).

Previous studies demonstrated that endolyn associates with CXCR4 after stimulation with CXCL12 and regulates downstream signaling with profound consequences on cell migration (Bae et al., 2008; Forde et al., 2007; Havens et al., 2006; Tang et al., 2012). The mechanism by which this regulation occurs remains unclear, although antibody inhibition experiments indicate that the N-terminal mucin-like domain of endolyn–not present in zebrafish endolyn–is required for this function (Forde et al., 2007). The CXCL12/CXCR4 axis is involved in cell proliferation, migration, adhesion and differentiation of various cell types, including kidney and other epithelial cells (Floege et al., 2009; Lu et al., 2009; Miller et al., 2008). Thus, endolyn may have a functional role in metanephric kidney that is mediated via CXCR4, e.g. during development or in renal tubule repair (Tögel et al., 2005; Ueland et al., 2009). A key step during pronephric kidney morphogenesis in zebrafish is the fluid flow-driven collective cell migration of epithelial cells starting around 30 hpf that is critical for generation of the proximal convoluted tubule (Vasilyev and Drummond, 2010; Vasilyev et al., 2009); however, endolyn-CXCR4 interaction is unlikely to be critically important for this event. While CXCR4 plays several important roles in zebrafish development, including migration of germ cells and lateral line primordial cells and muscle formation (Chong et al., 2007; Knaut et al., 2003; Perlin and Talbot, 2007; Valentin et al., 2007), no effects on pronephric kidney function have been reported in CXCR4 morphants. Moreover, the lack of gross morphological changes in the pronephric duct of endolyn morphants is inconsistent with major defects in cell migration, proliferation or apoptosis. Interestingly, Bae et al. found that overexpression of both wild type endolyn and the endocytosis-defective YA mutant promoted myoblast fusion, a CXCR4-mediated function, with the latter having an even stronger promyogenic activity (Bae et al., 2008). This suggests that endolyn has different cellular functions, some of which are only dependent on its surface expression, while others require active endocytosis. Future studies will be directed towards identifying additional interaction partners of endolyn and the mechanism(s) by which this protein affects endocytosis and vertebrate kidney function.

Materials and Methods

Zebrafish husbandry

All animal husbandry adheres to the National Institutes of Health Guide for the Care and Use of Laboratory Animals. Zebrafish were raised and maintained under standard conditions and staged as described previously (de Groh et al., 2010). Embryos were collected from group matings of wild-type AB adult zebrafish. Embryos were kept in E3 solution at 28.5℃. For *in situ* hybridization, embryos were kept in E3 solution containing 0.003% 1-pheny1-2-thiourea after 24 hpf.

Whole-mount *in situ* hybridization and immunocytochemistry

In situ hybridization was performed as described previously (de Groh et al., 2010). Full length endolyn cDNA was purchased from Open Biosystems. The endolyn anti-sense probe was made using the digoxigenin labelling kit (Roche) according to manufacturer's recommendations. T7 RNA polymerase was used for RNA synthesis after linearization of the endolyn cDNA with *Eco*RI. Embryos fixed in 4% PFA overnight at 4℃ were incubated with the endolyn anti-sense probe at 65℃, then washed extensively, incubated in 2% blocking reagent (Roche) with 5% sheep serum in MAB buffer (100 mM maleic acid and 150 mM NaCl), and incubated with anti-digoxigenin alkaline phosphatase antibody (Roche) at 1:15,000 dilution overnight at 4℃. BM purple AP substrate (Roche) was added for staining after extensive washing with PBS+0.1%Tween 20. Stained embryos were photographed using a Leica DMI 6000 CS Trino confocal microscope and images were processed using Adobe Photoshop.

RT-PCR

Dechorionated zebrafish embryos (~30 per stage) were homogenized with a plastic microcentrifuge pestle in 500 µl of TRI reagent (Ambion), and RNA was isolated using the RNeasy Micro Kit (Qiagen) according to the manufacturer's protocol. One µg of RNA was used for the synthesis of cDNA using M-MLV reverse transcriptase (Ambion) according to the manufacturer's recommendations. PCR was performed using the BioRad® icycler and GeneAmp® High Fidelity PCR System (Applied Biosystems). Primer sets against endolyn were designed using PrimerQuest on the IDT website (forward primer: 5′-ATGAGAACCAAACAGC-CAACTGCG−3′; reverse primer: 5′-CACACGCTGACAGACACAAACCAA-3′). The denaturing temperature was 95℃, the annealing temperature was 55℃, and the extension temperature was 68℃, with an amplification cycle of 30.

Embryo microinjection

A translational blocking MO against endolyn was designed and ordered from Gene Tools, LLC. (5′-TCACGGCGAAAAGTCTCCAAAACAT-3′), resuspended in nuclease free water (Ambion) at 20 mg/ml, and diluted to 1 mg/ml for microinjection. Zebrafish embryos were injected at up to the eight-cell stage with either the indicated doses of endolyn or control (scrambled) MO. Embryos were allowed to develop in E3 solution at 28.5℃. At 48 hpf, images were taken and embryo phenotypes classified. For rat endolyn rescue experiments, zebrafish embryos were injected at the one-cell stage with 100 pg of synthetic wild-type or mutant rat endolyn mRNA. Embryos were photographed and classified at 48 hpf to assess the extent of rescue.

Rhodamine-dextran clearance assay

Renal function was assayed as previously described (Cianciolo Cosentino et al., 2010). Briefly, 1 ng of 10 or 70 kDa Rhodamine-dextran was injected into the common cardinal vein of embryos injected with either control or endolyn MOs (and rescue mRNA constructs where indicated) at 48 hpf. Embryos were imaged under identical conditions sequentially at 1, 5 and 24 h post-injection. The loss of fluorescence near the common cardinal vein area was quantified using Adobe Photoshop. Statistical significance was assessed using the Mann–Whitney rank sum test.

Indirect immunofluorescence

Rat kidney: The preparation and labelling of rat kidney cryostat sections has been described (Rondanino et al., 2011). Sections were co-labelled with mouse mAb502 to endolyn (ascites 1:200) and polyclonal antibody 1637 to aminopeptidase N (serum 1:1000) (Ihrke et al., 2001; Ihrke et al., 1998), followed by Alexa488- or DyLight549-labelled anti-mouse and Cy3- or DyLight488-labelled anti-rabbit secondary antibodies (Molecular Probes and Jackson ImmunoResearch Laboratories, respectively). Optical sections (0.6–1.0 µm) were imaged with a Zeiss LSM 710 confocal microscope equipped with a 63×plan Plan apo objective and processed using NIH ImageJ and Adobe Photoshop software. Single sections

are shown in Fig. 1, and maximal projections of 12–14 sections corresponding to 5.5–6.5 μm tissue thickness are shown in supplementary material Fig. S1. *Zebrafish embryos:* Embryos were fixed with 4% paraformaldehyde for 4 h at ambient temperature and washed overnight with PBS. Embryos were incubated in increasing concentrations of sucrose up to 30% (w/v), mounted in Tissue Freezing Medium (Ted Pella) and frozen at −80℃. Tissue sections (12 μm thick) were cut using a cryostat (Leica CM1850), placed onto slides, and dried for 30 min at 37℃. Sections were blocked using 10% Normal Goat Serum and incubated with 3G8 antibody (European *Xenopus* Resource Centre at Portsmouth University; 1:100) overnight at 4℃. After extensive washing with PBS+0.1%Tween-20, sections were incubated with Alexa-488 conjugated secondary antibodies at 1:500 dilution. Sections were blocked again and incubated with a polyclonal antibody against rat endolyn (1:100; overnight at 4℃) followed by extensive washing and incubation with Alexa-568 conjugated secondary antibodies (1:500 dilution). For Na^+K^+-ATPase staining, embryos were fixed using Dent's fixative (80% methanol and 20% DMSO) for 4 h at room temperature as described in (Cianciolo Cosentino et al., 2010). Upon rehydration, embryos were incubated with sucrose and sectioned as previously described. After block with 10% Normal Goat Serum, sections were incubated with anti-Na^+K^+-ATPase antibody at 1:10 dilution overnight followed by extensive wash with PBS+0.1%Tween-20. Sections were then incubated with Alexa-568 conjugated secondary antibodies at 1:500 dilution. Upon dehydration, sections were mounted with Aqua Poly/Mount (Polysciences). Sections were imaged using a Leica DM6000B microscope with an HCX PL APO 40×/1.25 oil objective and acquired using a QImaging Retiga 4000R camera. *MDCK cells:* Filter grown cells were fixed by adding 4% paraformaldehyde at 37℃. Cells were permeabilized with 0.1% TX-100 in PBS for 10 min, blocked with 1% fish gelatin (Sigma), and incubated with mouse mAb502 against endolyn (ascites 1:500) and rat monoclonal antibody against ZO-1 (hybridoma supernatant from G. Apodaca, used neat) for 1 h. After extensive washing with PBS, filters were incubated with Alexa 488- and 647-conjugated secondary antibodies (Molecular Probes), washed, mounted, and imaged. Confocal stacks were collected and XZ images were generated and processed using MetaMorph.

Generation of mutant endolyn constructs

Generation of the rat endolyn YA mutant was previously described (Ihrke et al., 2001). The 4NA and TMD3 mutant constructs were generated by site-directed mutagenesis using PCR, subcloned into the pCB6 vector (Brewer and Roth, 1991), and verified by DNA sequencing. To obtain mRNA for rescue experiments, constructs were subcloned into pCS2+ vector behind the SP6 promoter. The mMESSAGE mMACHINE SP6 Kit (Ambion) was used to make mRNA from linearized cDNA.

Generation of MDCK stable cell lines

Stably transfected cell lines were generated in MDCK II cells as previously described (Weisz et al., 1992) and cultured in MEM with 10% fetal bovine serum and 400 μg/ml G418. For domain selective biotinylation and immunofluorescence experiments, cells were cultured on permeable supports for three days and then incubated with 2 mM butyrate for 18–21 h to induce endolyn expression.

Domain selective biotinylation of wild-type and mutant endolyn constructs

Polarized MDCK cells were starved and pulse-labelled for 2 h with [^{35}S]-cysteine, then chased for 1 h. Biotinylation was performed essentially as described previously (Altschuler et al., 2000). After cell lysis and immunoprecipitation with anti-endolyn antibody, samples were eluted. Four-fifths of the eluate was incubated overnight with streptavidin agarose (Pierce) to recover biotinylated proteins; the remainder was used to determine total endolyn. All samples were resolved on SDS-PAGE. Polarity was quantitated after exposure of dried gels to PhosphorImager screens.

Acknowledgements

We thank Núria Pastor-Soler for providing rat kidney cryostat sections.

Funding

This work was supported by the National Institutes of Health [grant number R01-DK54407 to O.A.W.]; a grant-in-aid award from the National Kidney Foundation [NKF/NCA to G.I.]; and the Urinary Tract Epithelial Imaging and Model Organisms Cores of the P30 Pittsburgh Center for Kidney Research [grant number NIH DK079307]. S.A.C. was funded by a Howard Hughes Medical Institute summer scholarship (HHMI 52006971). Deposited in PMC for release after 12 months.

Supplementary material available online at
http://jcs.biologists.org/lookup/suppl/doi:10.1242/jcs.111468/-/DC1

References

Altschuler, Y., Kinlough, C. L., Poland, P. A., Bruns, J. B., Apodaca, G., Weisz, O. A. and Hughey, R. P. (2000). Clathrin-mediated endocytosis of MUC1 is modulated by its glycosylation state. *Mol. Biol. Cell* **11**, 819-831.

Anzenberger, U., Bit-Avragim, N., Rohr, S., Rudolph, F., Dehmel, B., Willnow, T. E. and Abdelilah-Seyfried, S. (2006). Elucidation of megalin/LRP2-dependent endocytic transport processes in the larval zebrafish pronephros. *J. Cell Sci.* **119**, 2127-2137.

Bae, G. U., Gaio, U., Yang, Y. J., Lee, H. J., Kang, J. S. and Krauss, R. S. (2008). Regulation of myoblast motility and fusion by the CXCR4-associated sialomucin, CD164. *J. Biol. Chem.* **283**, 8301-8309.

Brewer, C. B. and Roth, M. G. (1991). A single amino acid change in the cytoplasmic domain alters the polarized delivery of influenza virus hemagglutinin. *J. Cell Biol.* **114**, 413-421.

Chong, S. W., Nguyet, L. M., Jiang, Y. J. and Korzh, V. (2007). The chemokine Sdf-1 and its receptor Cxcr4 are required for formation of muscle in zebrafish. *BMC Dev. Biol.* **7**, 54.

Cianciolo Cosentino, C., Roman, B. L., Drummond, I. A. and Hukriede, N. A. (2010). Intravenous microinjections of zebrafish larvae to study acute kidney injury. *J. Vis. Exp.* **42**, 2079.

Cresawn, K. O., Potter, B. A., Oztan, A., Guerriero, C. J., Ihrke, G., Goldenring, J. R., Apodaca, G. and Weisz, O. A. (2007). Differential involvement of endocytic compartments in the biosynthetic traffic of apical proteins. *EMBO J.* **26**, 3737-3748.

de Groh, E. D., Swanhart, L. M., Cosentino, C. C., Jackson, R. L., Dai, W., Kitchens, C. A., Day, B. W., Smithgall, T. E. and Hukriede, N. A. (2010). Inhibition of histone deacetylase expands the renal progenitor cell population. *J. Am. Soc. Nephrol.* **21**, 794-802.

Devonald, M. A., Smith, A. N., Poon, J. P., Ihrke, G. and Karet, F. E. (2003). Non-polarized targeting of AE1 causes autosomal dominant distal renal tubular acidosis. *Nat. Genet.* **33**, 125-127.

Doyonnas, R., Yi-Hsin Chan, J., Butler, L. H., Rappold, I., Lee-Prudhoe, J. E., Zannettino, A. C., Simmons, P. J., Bühring, H. J., Levesque, J. P. and Watt, S. M. (2000). CD164 monoclonal antibodies that block hemopoietic progenitor cell adhesion and proliferation interact with the first mucin domain of the CD164 receptor. *J. Immunol.* **165**, 840-851.

Drummond, I. A. (2005). Kidney development and disease in the zebrafish. *J. Am. Soc. Nephrol.* **16**, 299-304.

Drummond, I. A. and Davidson, A. J. (2010). Zebrafish kidney development. *Methods Cell Biol.* **100**, 233-260.

Eitner, F., Cui, Y., Hudkins, K. L. and Alpers, C. E. (1998). Chemokine receptor (CXCR4) mRNA-expressing leukocytes are increased in human renal allograft rejection. *Transplantation* **66**, 1551-1557.

Floege, J., Smeets, B. and Moeller, M. J. (2009). The SDF-1/CXCR4 axis is a novel driver of vascular development of the glomerulus. *J. Am. Soc. Nephrol.* **20**, 1659-1661.

Forde, S., Tye, B. J., Newey, S. E., Roubelakis, M., Smythe, J., McGuckin, C. P., Pettengell, R. and Watt, S. M. (2007). Endolyn (CD164) modulates the CXCL12-mediated migration of umbilical cord blood CD133+ cells. *Blood* **109**, 1825-1833.

Havens, A. M., Jung, Y., Sun, Y. X., Wang, J., Shah, R. B., Bühring, H. J., Pienta, K. J. and Taichman, R. S. (2006). The role of sialomucin CD164 (MGC-24v or endolyn) in prostate cancer metastasis. *BMC Cancer* **6**, 195.

Hentschel, D. M., Park, K. M., Cilenti, L., Zervos, A. S., Drummond, I. and Bonventre, J. V. (2005). Acute renal failure in zebrafish: a novel system to study a complex disease. *Am. J. Physiol. Renal Physiol.* **288**, F923-F929.

Ihrke, G., Martin, G. V., Shanks, M. R., Schrader, M., Schroer, T. A. and Hubbard, A. L. (1998). Apical plasma membrane proteins and endolyn-78 travel through a subapical compartment in polarized WIF-B hepatocytes. *J. Cell Biol.* **141**, 115-133.

Ihrke, G., Gray, S. R. and Luzio, J. P. (2000). Endolyn is a mucin-like type I membrane protein targeted to lysosomes by its cytoplasmic tail. *Biochem. J.* **345**, 287-296.

Ihrke, G., Bruns, J. R., Luzio, J. P. and Weisz, O. A. (2001). Competing sorting signals guide endolyn along a novel route to lysosomes in MDCK cells. *EMBO J.* **20**, 6256-6264.

Ihrke, G., Kyttälä, A., Russell, M. R., Rous, B. A. and Luzio, J. P. (2004). Differential use of two AP-3-mediated pathways by lysosomal membrane proteins. *Traffic* **5**, 946-962.

Jones, J., Otu, H., Spentzos, D., Kolia, S., Inan, M., Beecken, W. D., Fellbaum, C., Gu, X., Joseph, M., Pantuck, A. J. et al. (2005). Gene signatures of progression and metastasis in renal cell cancer. *Clin. Cancer Res.* **11**, 5730-5739.

Julenius, K., Mølgaard, A., Gupta, R. and Brunak, S. (2005). Prediction, conservation analysis, and structural characterization of mammalian mucin-type O-glycosylation sites. *Glycobiology* **15**, 153-164.

Knaut, H., Werz, C., Geisler, R. The Tübingen 2000 Screen Consortium and Nüsslein-Volhard, C. (2003). A zebrafish homologue of the chemokine receptor Cxcr4 is a germ-cell guidance receptor. *Nature* **421**, 279-282.

Lee, Y. N., Kang, J. S. and Krauss, R. S. (2001). Identification of a role for the sialomucin CD164 in myogenic differentiation by signal sequence trapping in yeast. *Mol. Cell. Biol.* **21**, 7696-7706.

Lu, B. C., Cebrian, C., Chi, X., Kuure, S., Kuo, R., Bates, C. M., Arber, S., Hassell, J., MacNeil, L., Hoshi, M. et al. (2009). Etv4 and Etv5 are required downstream of GDNF and Ret for kidney branching morphogenesis. *Nat. Genet.* **41**, 1295-1302.

Miller, R. J., Banisadr, G. and Bhattacharyya, B. J. (2008). CXCR4 signaling in the regulation of stem cell migration and development. *J. Neuroimmunol.* **198**, 31-38.

Perlin, J. R. and Talbot, W. S. (2007). Signals on the move: chemokine receptors and organogenesis in zebrafish. *Sci. STKE* **2007**, pe45.

Potter, B. A., Ihrke, G., Bruns, J. R., Weixel, K. M. and Weisz, O. A. (2004). Specific N-glycans direct apical delivery of transmembrane, but not soluble or glycosylphosphatidylinositol-anchored forms of endolyn in Madin-Darby canine kidney cells. *Mol. Biol. Cell* **15**, 1407-1416.

Potter, B. A., Weixel, K. M., Bruns, J. R., Ihrke, G. and Weisz, O. A. (2006). N-glycans mediate apical recycling of the sialomucin endolyn in polarized MDCK cells. *Traffic* **7**, 146-154.

Rondanino, C., Poland, P. A., Kinlough, C. L., Li, H., Rbaibi, Y., Myerburg, M. M., Al-bataineh, M. M., Kashlan, O. B., Pastor-Soler, N. M., Hallows, K. R. et al. (2011). Galectin-7 modulates the length of the primary cilia and wound repair in polarized kidney epithelial cells. *Am. J. Physiol. Renal Physiol.* **301**, F622-F633.

Swanhart, L. M., Cosentino, C. C., Diep, C. Q., Davidson, A. J., de Caestecker, M. and Hukriede, N. A. (2011). Zebrafish kidney development: basic science to translational research. *Birth Defects Res. C Embryo Today* **93**, 141-156.

Tang, J., Zhang, L., She, X., Zhou, G., Yu, F., Xiang, J. and Li, G. (2012). Inhibiting CD164 Expression in Colon Cancer Cell Line HCT116 Leads to Reduced Cancer Cell Proliferation, Mobility, and Metastasis in vitro and in vivo. *Cancer Invest*. **30**, 380-389.

Tögel, F., Isaac, J., Hu, Z., Weiss, K. and Westenfelder, C. (2005). Renal SDF-1 signals mobilization and homing of CXCR4-positive cells to the kidney after ischemic injury. *Kidney Int.* **67**, 1772-1784.

Ueland, J., Yuan, A., Marlier, A., Gallagher, A. R. and Karihaloo, A. (2009). A novel role for the chemokine receptor Cxcr4 in kidney morphogenesis: an in vitro study. *Dev. Dyn.* **238**, 1083-1091.

Valentin, G., Haas, P. and Gilmour, D. (2007). The chemokine SDF1a coordinates tissue migration through the spatially restricted activation of Cxcr7 and Cxcr4b. *Curr. Biol.* **17**, 1026-1031.

Vasilyev, A. and Drummond, I. A. (2010). Fluid flow and guidance of collective cell migration. *Cell Adh. Migr.* **4**, 353-357.

Vasilyev, A., Liu, Y., Mudumana, S., Mangos, S., Lam, P. Y., Majumdar, A., Zhao, J., Poon, K. L., Kondrychyn, I., Korzh, V. et al. (2009). Collective cell migration drives morphogenesis of the kidney nephron. *PLoS Biol.* **7**, e9.

Weisz, O. A., Machamer, C. E. and Hubbard, A. L. (1992). Rat liver dipeptidylpeptidase IV contains competing apical and basolateral targeting information. *J. Biol. Chem.* **267**, 22282-22288.

Wingert, R. A. and Davidson, A. J. (2008). The zebrafish pronephros: a model to study nephron segmentation. *Kidney Int.* **73**, 1120-1127.

Zannettino, A. C., Bühring, H. J., Niutta, S., Watt, S. M., Benton, M. A. and Simmons, P. J. (1998). The sialomucin CD164 (MGC-24v) is an adhesive glycoprotein expressed by human hematopoietic progenitors and bone marrow stromal cells that serves as a potent negative regulator of hematopoiesis. *Blood* **92**, 2613-2628.